Intelligent Recognition of Subcarrier for Wireless Link of Satellite Communication

Mingxiang Guan, Le Wang

School of Electronic Communication Technology, Shenzhen Institute of Information Technology, China
gmx2020@126.com,wangle@sziit.edu.cn

Abstract

An intelligent recognition algorithm for subcarrier based on combining Fourier transform wavelet and multi-resolution analysis was proposed in the paper. The proposed method can recognize each component from the mixed signal fast and accurately. Also the recognized signals were identified based on the estimations of subcarrier code rate and frequency. The proposed subcarrier recognition method can effectively recognize multiple signals from the subcarrier signal according to the simulation results. Moreover, the method exhibits the advantages of high recognition precision and strong noise immunity.

Keywords: Satellite communication, Subcarrier, Recognition

1 Introduction

Recently, there are two kinds of methods to detect the multiple signals in a frequency band. One method is the manual and the other is the electric scanning [1-2]. By the manual method, the multiple signals are separated based on the observations of the distribution of frequency spectrum through tuning and filtering manually. Due to the false detection rates and low miss, the Manual method prevails in practical applications in the simple communication system. Because it is always slow, labor-intensive and low-efficiency, it is not appropriate for the complex and advanced communication system [3-6]. In order to resolve the manual method, electric scanning method was proposed [7-8]. By using the computer and performing automatic detection, the electric scanning method analyzes the signal' spectral characteristics and separates the mixed signals through certain algorithms [9-10]. The electric scanning method generally performs false detection rates and high miss. In a certain number of unknown signals which are mutually independent, such the mixed signals should be investigated by using electric scanning. Because both the transmission characteristics and signal sources are unknown, blind separation method based on the difference among the received signals was proposed [11]. Using spatial filtering and antenna array receiving system to achieve the separation of multiple signals, then these problems are resolved and known as blind separation [12-13]. Due to the signal bandwidth is uncertain and the number of the mutually independent signals is unknown, an appropriate detection and separation method for the mixed signals is lacked [14-15].

Separation of the signals with uncertain bandwidth, signal number and separable frequency spectra was focused in the article. Also an intelligent recognition algorithm for subcarrier based on combining Fourier transform wavelet and multi-resolution analysis and Fourier transform was proposed in the paper. The proposed method can recognize each component from the mixed signal fast and accurately. Also the recognized signals were identified based on the estimations of subcarrier code rate and frequency. The proposed subcarrier recognition method can effectively recognize multiple signals from the subcarrier signal according to the simulation results. Moreover, the method exhibits the advantages of high recognition precision and strong noise immunity.

2 δ_1 and δ_2 Selection Based on Wavelet Analysis

2.1 Principle of Wavelet Analysis

According to literature [16], For the signal to be separated $s(t)$ in which the frequency spectra of each mixed signals do not overlap mutually. FFT at Point M can be written as:

$$s(k)=\sum_{n=0}^{M-1}s(n)e^{-j2\pi k/M}(0\le k\le M-1) \quad \textbf{(1)}$$

Then, the power spectral density (PSD) of $s(n)$ can be achieved by:

$$p(k)=s(k)\times\overline{s(k)},(0\le k\le M-1) \quad \textbf{(2)}$$

*Corresponding Author: Mingxiang Guan; E-mail: gmx2020@126.com
DOI: 10.3966/160792642019102006017

where the symbol of '-' represents the complex conjugate operation.

Wavelet multi-resolution analysis was proposed by S. Mallat in constructing the orthogonal wavelet basis. S. Mallat also developed the wavelet multi-resolution algorithm for signals, also known as Mallat algorithm. Figure 1 illustrates the wavelet multi-resolution analysis structure of the signal $s(t)$ on three different decomposition levels, in which A_i and D_i denote the obtained coarse-resolution approximation and detail information of $s(t)$ on the decomposition level i. In the wavelet multi-resolution analysis, as the decomposition level i increased, the high-frequency information included in the coarse-resolution approximation A_i of $s(t)$ gradually decreased, which was further rejected in the decomposition on the next level. After the decomposition level by level, only the development tendency of the signal, namely, the signal's rough outline, was remained in A_i, which represents the low-frequency information of $s(t)$. Accordingly, the burrs induced by noise or the violent vibration components of the signal itself were filtered as the high-frequency information.

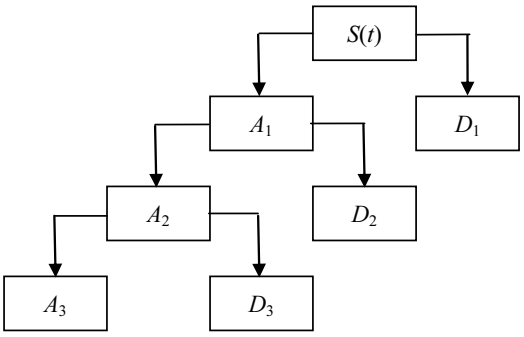

Figure 1. Illustration of the wavelet multi-resolution analysis process on the signal $s(t)$

2.2 Selection of δ_1 and δ_2

After wavelet multi-resolution analysis and processing, the high-frequency information was gradually rejected from the coarse-resolution approximation of the power spectrum $P_s(\omega)$ of the noisy communication signal $s(t)$, and only the low-frequency information was left eventually. On an appropriate decomposition level i, the burrs or the violent violent components of the power spectrum $P_s(\omega)$ were effectively removed and the obtained coarse-resolution approximation A_i favorably reflected the rough outline of $P_s(\omega)$. Moreover, the number of data in A_i was far less than that in $P_s(\omega)$. As stated above, the frequency of each mixed signal in noisy communication signal $s(t)$ were non-overlapped. For the coarse-resolution approximation A_i of the power spectrum $P_s(\omega)$ on a certain decomposition level i, the number of signals in $s(t)$ could be rapidly and accurately determined using a simple program.

After the determination of the number of mixed signals N in the communication signal, the adaptive selection algorithm of δ_1 and δ_2, two threshold values in the above-described two-step signal separation algorithm, was designed as follows.

Assuming that the power spectrum of the communication signal $s(t)$ is defined as $P_s(\omega)$ and the mean value of $P_s(\omega)$ is m, let $\delta_1 = m$ and $\delta_2 = m$ at the beginning, we then conducted a two-step signal separation on $P_s(\omega)$, and the following expressions were acquired:

$$\text{If } N > N_0,\ \delta_1' = \delta_1 + \Delta\delta_1 \text{ and } \delta_2' = \delta_2 + \Delta\delta_2;$$
$$\text{If } N < N_0,\ \delta_1' = \delta_1 - \Delta\delta_1 \text{ and } \delta_2' = \delta_2 - \Delta\delta_2'.$$

where $\Delta\delta_2$ and $\Delta\delta'$ are the corrected values of δ_2.

For the reset thresholds δ_1 and δ_2, we also conducted the two-step signal separation on $P_s(\omega)$. If $\tilde{N}' \neq N$ (where $\tilde{N}'$ denotes the number of separated signals), the values of δ_1 and δ_2 were readjusted. The above-described signal separation was repeated until the number of separated signal equals to N. Accordingly, not only could δ_1 and δ_2 be adaptively determined, but also could the power spectra of each mixed signals and the beginning and destination frequency points in the frequency band be separated from the power spectrum $P_s(\omega)$ of the communication signal $s(t)$.

It should be noted that δ_1 always equaled to m so that no error was produced in the separation of communication signal. Actually, since the frequency of each mixed signal did not overlap with each other, the reasonability of the value of δ_1 was easily discussed.

3 Wireless Link Recognition

3.1 Estimation of the Subcarrier Frequency

Then we conducted zero-cross detection on the signal $r(n)$. If $r(n_i)$ and $r(n_i+1)$ have different signs, it can be regarded that zero point exists in the time period of $(n/f_s, (n+1)/f_s)$. The position of zero point can be calculated by the following linear interpolation formula:

$$\alpha(i) = \frac{1}{f_s}\left[n_i + \frac{r(n_i)}{r(n_i) - r(n_i+1)}\right] \quad i = 1, 2, \cdots, M_z \qquad \textbf{(3)}$$

where M_z denotes the number of detected zero points. By defining that the first difference sequence of $\{\alpha(i)\}$

is a zero-cross interval sequence $\{y(i)\}$, the following expression can be obtained:

$$y(i)=r(i+1)-r(i)\quad i=1,2,\cdots,M_z-1 \tag{4}$$

The position of the *i*-th zero point in the sinusoidal signal of noise can be written as:

$$\alpha(i)=\frac{i\pi-\frac{\pi}{2}}{2\pi f_c}+\xi(i)=\frac{i-0.5}{2f_c}+\xi(i)\quad i=1,2,\cdots,M_z-1 \tag{5}$$

where $\xi(i)$ denotes the independent identically distributed (IID) random variable introduced by noise and measuring errors. Then, Eq. (5) can be rewritten as:

$$\begin{aligned}&y(i)=\frac{1}{2f_c}+\varepsilon(i)\\&\varepsilon(i)=\xi(i+1)-\xi(i)\ \ i=1,2,\cdots,M_z-1\end{aligned} \tag{6}$$

where $\varepsilon(i)$ approximately follows the zero-mean normal distribution. Thus, $\mathrm{E}[y(i)]=\frac{1}{2f_c}$, and the formula for estimating the subcarrier frequency at zero point can be written as:

$$f_c=\frac{M_z-1}{2\sum_{i=1}^{M_z-1}y(i)} \tag{7}$$

3.2 Estimation of the Code Rate of Subcarrier

For the digital modulation signal, the information is loaded to the instantaneous characteristics. For the MASK signal, the digital information is loaded to the instantaneous phase $\phi_{NL}(n)$; for the MFSK signal, the digital information is loaded to the instantaneous frequency $f(n)$; for the QAM signal, the digital information is loaded to both instantaneous amplitude and frequency. All these instantaneous characteristics can be described by the corresponding waveform of the pulse amplitude modulation that carries the digital information, denotes as $W(n)$. The *L*-order difference of $W(n)$ was then calculated and the absolute value was used:

$$\begin{aligned}&W_1(n)=\left|W(n+L)-W(n)\right|\\&n=0,1,\cdots,N-L-1\end{aligned} \tag{8}$$

Then, the mean value of $W_1(n)$ was calculated by:

$$m_w=\frac{1}{N-L}\sum_{i=0}^{N-L-1}W_1(i) \tag{9}$$

Then, the sequence $W_1(n)$ was judged using m_w as the threshold. If $W_1(n)>m_w$, $W_1(n)$ was judged to be 1; otherwise, $W_1(n)$ was judged to be 0. The serial numbers of the elements that exceeded m_w were recorded, and the following sequence $\{h(i)\}$ was obtained:

$$\{h(i)\}=\{n\,|\,W_1(n)>m_w\} \tag{10}$$

$\{h(i)\}$ represent the sequence of the positions where the phase steps of $W(n)$ occurred. Each step point in $\{h(i)\}$ showed up a step band with a width of L. Using the center of step band as the turning point of code elements, the sequence of the converted positions of code elements $\{h_c(i)\}$ was acquired. The first-order difference sequence of $\{h_c(i)\}$ was then calculated by:

$$N_d \tag{11}$$

where N_d denotes the length of the sequence $\{h_{cd}(i)\}$. Let $N_m=\min[h_{cd}(n)]$ and $n_h(i)=\mathrm{round}\left[\frac{h_{cd}(i)}{N_m}\right]$, the average distance between code elements N_s can be written as:

$$N_s=\frac{\sum_{i=1}^{N_d}h_{cd}(i)}{\sum_{i=1}^{N_d}n_h(i)} \tag{12}$$

Accordingly, the code element rate can be estimated by:

$$\hat{r}_s=\frac{f'_s}{N_s} \tag{13}$$

where f'_s denotes the input rate of data.

4 Verification

The frequency spectrum varies with the modulation index *h* in the FSK modulated signal. The frequency spectrum is a single-peak continuous spectrum with the carrier frequency as the center in the PSK modulated signal. Two frequencies of FSK Assumed are defined as f_1 and f_2. Assuming that the bit rate is R_s, the *h* is modulation index which can be achieved by $h=|f_2-f_1|/R_s$.

The separation processing was described in the following.

Step 1. Assuming that blind communication signal $s(t)$ and the power spectrum of $s(t)$, defined as $P_s(\omega)$.

Step 2. Conduct discrete orthogonal wavelet transform (DWT) on $P_s(\omega)$ based on wavelet multi-resolution analysis. Coarse approximation of $P_s(\omega)$ on a certain decomposition level *i* and the reconstructed signal was obtained and defined as A_i A_i and RA_i.

Step 3. The number of the mixed signals based on A_i, defined as N_0.

Step 4. δ_1 and δ_2 as the initial thresholds equal to m, i.e., $\delta_1 = \delta_2 = m$,where the mean value of $P_s(\omega)$ was m . After coarse separation, blind channel separation on the reconstructed signal RA_i of $s(t)$ was assumed

Step 5. Conduct adjustment on δ_1 and δ_2 . The specific process is described below.

If $N > N_0$, $\delta_1' = \delta_1 + \Delta\delta_1$ and $\delta_2' = \delta_2 + \Delta\delta_2$;

If $N < N_0$, $\delta_1' = \delta_1 - \Delta\delta_1^{'}$ and $\delta_2' = \delta_2 - \Delta\delta_2'$.

where N defines the number of separated channels; $\Delta\delta_1$, $\Delta\delta_1^{'}$, $\Delta\delta_2$ and $\Delta\delta_2'$ are the corrected values of δ_1 and δ_2 .

Step 6. Reconstructed signal RA_i of $s(t)$ in the blind channel for the coarse resolution approximation separation using the corrected thresholds δ_1' and δ_2'.

Step 7. If $N' \neq N_0$ (where N' defines the number of separated signals), the process repetition until the number of blind channels equals to N_0 from the Step 5. From the power spectrum $P_s(\omega)$, in the frequency band the power spectrum of each blind channel was acquired at the destination points.

Step 8. The corresponding filter and separation of the mixed signals $s_1(t), s_2(t), \cdots, s_N(t)$ from $s(t)$ were operated. In accordance with procedures the simulations were performed. We set the values of δ_1 were set as zero which are correct, i.e., $\Delta\delta_1 = 0$ and $\Delta\delta_1^{'} = 0$. Set the values of δ_2 as $0.01m$ and $0.005m$, respectively which are correct, $\Delta\delta_2 = 0.01m$ and $\Delta\delta_2' = 0.005m$, the mean value of $P_s(\omega)$ was m. Figure 2 and Figure 3 display the simulation results.

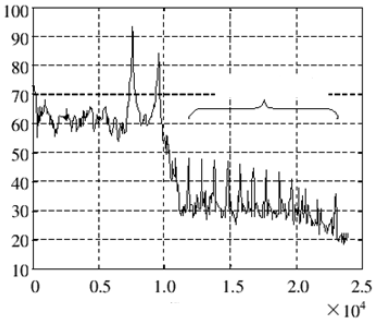

Figure 2. $P_s(\omega)$ of $s(t)$ power spectrum

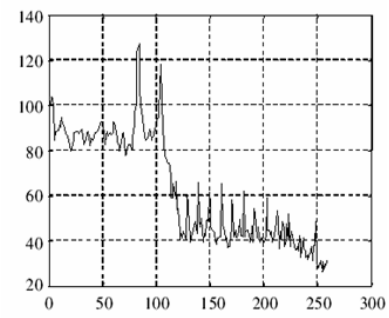

(a) Coarse approximation of $P_s(\omega)$ for A1

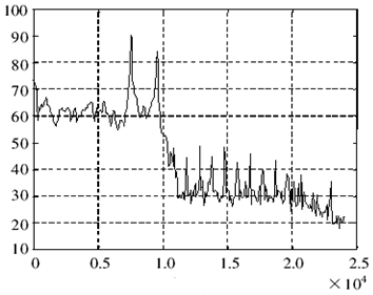

(b) Reconstructed signal RA_1

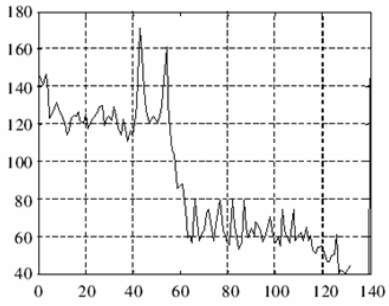

(c) Coarse approximation of $P_s(\omega)$ for A2

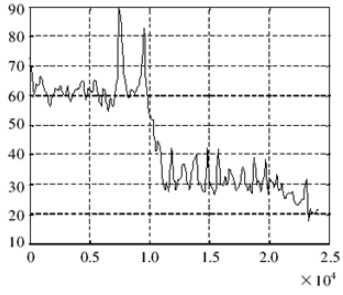

(d) Reconstructed signal RA_2

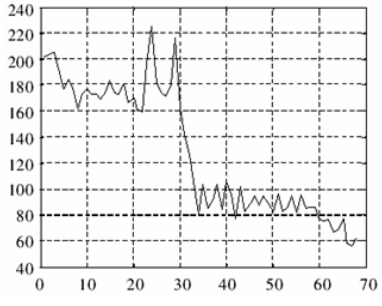

(e) Coarse approximation of $P_s(\omega)$ for A3

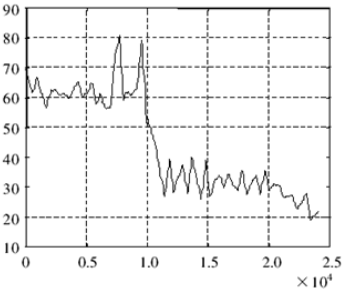

(f) Reconstructedsignal RA_3

Figure 3. Separation process of the subcarriers

To make the simulation results more universal, two modulation modes, phase shift keying (PSK) and frequency shift keying (FSK), were used for two subcarriers. In the present study, the subcarrier modulation on satellite up-links were taken as the example. Assuming that the frequencies of two subcarriers were 8 kHz and 16 kHZ (f_{sc1} = 8kHz and f_{sc2} = 16kHz), respectively, the sine wave with a frequency of 100 kHz (f_t=100kHz) was used as the ranging sidetone, the code rate was set as 1 kbps (R_s=1kbps) and the powers of each subcarriers exhibited no obvious differences. Figure 4 displays the frequency spectrum of the modulated satellite subcarrier signal before and after partition, in which SNR and the FSK modulation index (h) were 3 dB and 0.6, respectively, and two subcarriers and one ranging sidetone were included.

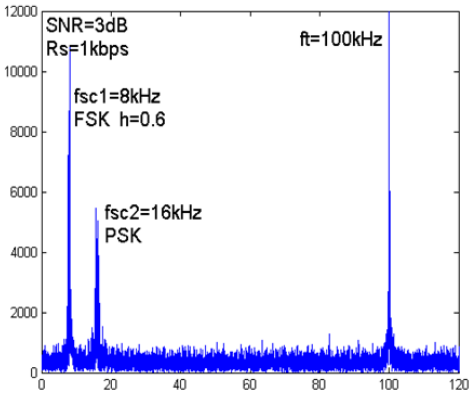

(a) Before partition

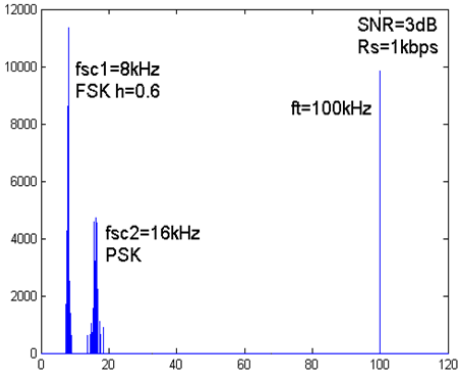

(b) after partition

Figure 4. Frequency spectrum of the subcarrier signal on the satellite communication link

For the convenience of analysis, Figure 5 displays some partial enlarged details of Fig. 4 and focused on the partition of two subcarriers. It can be observed that, adequate zero points were acquired between two subcarriers after partition under the given conditions, which could be taken as the basis for partition.

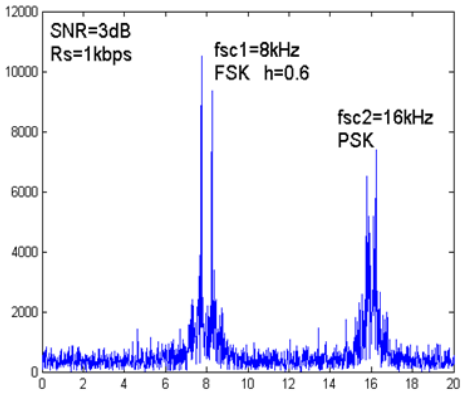

(a) Before partition

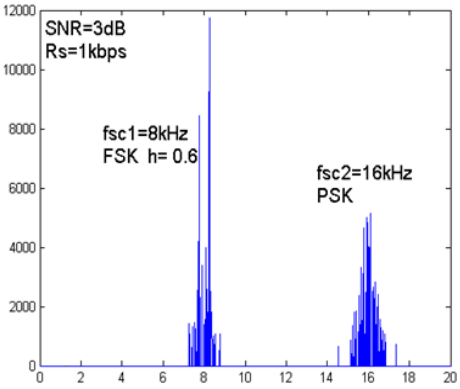

(b) after partition

Figure 5. Partial enlarged details of the frequency spectrum of the subcarrier signal on the satellite communication link

According to the simulation results, the decrease of SNR and the increase of FSK modulation index could lead to a poorer partition. As shown in Figure 6, when SNB < 0 dB, insufficient zero points existed between two subcarriers and thus the partition could not be realized using the proposed zero-point-based partition method.

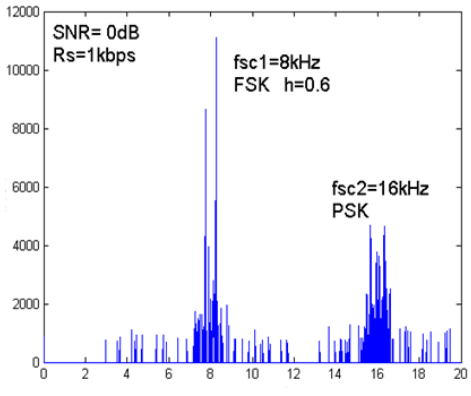

Figure 6. Signal partition results when SNR = 0 dB

When the code rate is 1 kbps and h exceeds 5, an error occurred in signal partition using the proposed method. As shown in Figure 7, when $h = 5$, the interval between two frequencies in FSK modulation was calculated by: $|f_2 - f_1| = 5 \times R_s = 5\text{kHz}$, and the frequency interval of two subcarriers was 8 kHz. Then, after partition, many zero points appeared between f_1 and f_2 and thus affected the normal subcarrier separation. Therefore, at a large h, an error would occur in the partition of subcarriers using the proposed zero-point-based method even for a large SNR. This is due to the fact that the proposed method was derived from the method of separating two FSK subcarriers and thus has certain limitations. According to the requirement, the FSK modulation index can not be too large. It means that we should pay more attention to the application range of the proposed zero-point-based partition method in practical use.

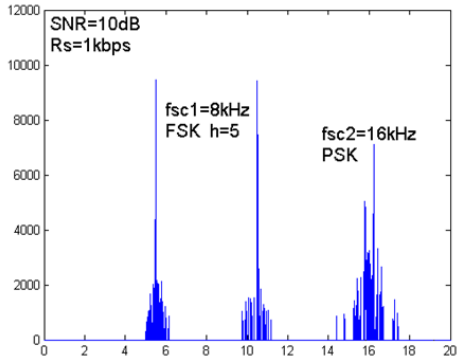

Figure 7. Signal partition results when $h = 5$

Actually, when $h < 0.5$, a single peak can be observed at the carrier frequency of FSK, and the frequency spectrum shows smooth roll-offs on its two sides. As h increased, the frequency spectrum of signal expanded and became concentrated towards f_1 and f_2. When $h > 0.7$, two peaks appeared; when $h = 1$, these two peaks were separated from each other and two discrete spectra appeared at f_1 and f_2, respectively. As h further increased, a certain amount of peaks were observed between f_1 and f_2, and zero-points occurred in the frequency spectrum in this range. As h increased and exceeded to a certain value ($h > 2$), would enter the high-index modulation, and the frequency spectrum would expand to an extremely wide spectrum. The FSK modulation with a small modulation index is preferred for the narrow-band channels since it occupies a narrow frequency band and thus exhibits a high band utilization rate.

Conclusively, when SNR $\geq$ 0 dB and h $\leq$ 5, the proposed zero-point-based partition method is applicable to simple subcarrier partitions. Moreover, the channel number of subcarriers can also be acquired. The method has simple principle but is easily to realize. After partition, each subcarriers can be separated by the filter for further modulation.

5 Conclusions

Fourier transform and Wavelet multi-resolution analysis was combined in the paper. In order to recognize the subcarrier signals with uncertain bandwidth, signal number and non-overlapped frequency spectrum of mixed signals, an intelligent recognition algorithm for subcarrier based on combining Fourier transform and Wavelet multi-resolution analysis was proposed in the paper. The proposed method can recognize each component from the mixed signal fast and accurately. Also the recognized signals were identified based on the estimations of subcarrier code rate and frequency. The proposed subcarrier recognition method can effectively recognize multiple signals from the subcarrier signal according to the simulation results. Moreover, the method exhibits the advantages of high recognition precision and strong noise immunity.

Acknowledgements

This paper is supported by the Guangdong Province higher vocational colleges & schools PearlRiver scholar funded scheme (2016), the project of Shenzhen Science and Technology Innovation Committee (JCYJ 20170817114522834, JCYJ20160608151239996), Key laboratory of Longgang District (LGKCZSYS2018 000028), the science and technology development center of Ministry of Education of China (2017A15009) and Engineering Applications of Artificial Intelligence Technology Laboratory (PT201701).

Reference

[1] Y. Zhou, X. Hu, T. Ke, Z. Tang, Ambiguity Mitigating Technique for Cosine-Phased Binary Offset Carrier Signal, *IEEE Transactions on Wireless Communications*, Vol. 11, No. 6, pp. 1981-1984, June, 2012.

[2] W. Dang, M. Tao, H. Mu, J. Huang, Subcarrier-pair Based Resource Allocation for Cooperative Multi-Relay OFDM Systems, *IEEE Transactions on Wireless Communications*, Vol. 9, No. 5, pp. 1640-1649, May, 2010.

[3] H.-C. Ting, R.-S. Chang, Improving the Performance of Broadcasting in Ad Hoc Wireless Networks, *Journal of Internet Technology*, Vol. 4, No. 4, pp. 209-216, October, 2003.

[4] S.-C. Yeh, J.-S. Wu, Performance Improvement and Analysis for Multimedia Transmission Services based on Wireless Networks, *Journal of Internet Technology*, Vol. 2, No. 1, pp. 33-38, January, 2001.

[5] H. Lee, K.-J. Lee, H. Kim, I. Lee, Resource Allocation Techniques for Wireless Powered Communication Networks With Energy Storage Constraint, *IEEE Transactions on Wireless Communications*, Vol. 15, No. 4, pp. 2619-2628, April, 2016.

[6] X. Jin, J. Zhang, Introduction on Application of Satellite Communications in High Speed Railway System, *Journal of Internet Technology*, Vol. 10, No. 4, pp. 381-384, August, 2009.

[7] D. Borio, Double Phase Estimator: New Unambiguous Binary Offset Carrier Tracking Algorithm, *IET Radar, Sonar & Navigation*, Vol. 8, No. 7, pp. 729-741, August, 2014.

[8] N. C. Shivaramaiah, A. G. Dempster, C. Rizos, Time-Multiplexed Offset-carrier QPSK for GNSS, *IEEE Transactions on Aerospace and Electronic Systems*, Vol. 49, No. 2, pp. 1119-1138, April, 2013.

[9] L. Guo, F. Yin, M. Lu, Overview on NBI Suppression of DSSS/CDMA Systems, *Chinese Journal of Electronics*, Vol. 37, No. 10, pp. 2248-2257, October, 2009.

[10] D. Borio, M. Rao, C. O'Driscoll, Codeless Processing of Binary Offset Carrier Modulated Signals, *IET Radar, Sonar & Navigation*, Vol. 7, No. 2, pp. 143-152, February, 2013.

[11] Z. Yao, J. Zhang, M. Lu, ACE-BOC: Dual-frequency Constant Envelope Multiplexing for Satellite Navigation, *IEEE Transactions on Aerospace and Electronic Systems*, Vol. 52, No. 1, pp. 466-485, February, 2016

[12] X. Ren, H. Xu, Z. Huang, F. Wang, F. Lu, Fast-ICA Based Optimize Blind Estimation of Spreading Sequence of CDMA signals, *Chinese Journal of Electronics*, Vol. 40, No. 8, pp. 1532-1538, August, 2012.

[13] N. H. Tran, H. H. Nguyen, T. Le-Ngoc, Subcarrier Grouping for OFDM with Linear Constellation Precoding over Multipath Fading Channels, *IEEE Transactions on Vehicular Technology*, Vol. 56, No. 6, pp. 3607-3613, September, 2007.

[14] Y. He, G. Cui, P. Li, R. Chang, W. Wang, Timing Advanced Estimation Algorithm of Low Complexity Based on DFT Spectrum Analysis for Satellite System, *China Communications*, Vol. 12, No. 4, pp. 140-150, April, 2015.

[15] Y. Zhang, W. Lu, H. Chen, D. Yu, Insight to Double Estimator Technique: The Concept of Subcarrier Aided Code Tracking, *2015 International Conference on Communications and Signal Processing (ICCSP)*, Melmaruvathur, India, 2015, pp. 163-167.

[16] M. Guan, L. Wang, B. Peng, Adaptive Separation of Subcarrier for Wireless Link of Satellite Communication, *Wireless Personal Communications*, Vol. 103, No. 1, pp. 159-166, November, 2018.

Biographies

Mingxiang Guan, who was born in Gong'an, Hubei, China in 1979, received his bachelor of Electronic Engineering from HUST, China, in 2002 and his master and Ph.D. of Communication Engineering from HIT, China, in 2004, 2008 respectively. His main interests are in the areas of wireless communication, HAPS communication and network communication research.

Le Wang, who was born in Jilin, China in 1979, received her bachelor, master and Ph.D. of Communication Engineering from Harbin Institute of Technology, China, in 2001, 2004 and 2010 respectively. Her main interests are in the areas of wireless communication and satellite communication research.